Int. J. Electrochem. Sci., 16 **(2021)** Article ID: 210329, doi: 10.20964/2021.03.61

International Journal of
ELECTROCHEMICAL
SCIENCE
www.electrochemsci.org

Transparent Dye-sensitized Module for Solar Windows

Lia Muliani[*], *Jojo Hidayat, Shobih, Natalita Maulani Nursam, Erlyta Septa Rosa,*
Putri Nur Anggraini, Lilis Retnaningsih.

Research Center for Electronic and Telecommunication, Indonesian Institute of Sciences (LIPI), Bandung, 40135, Indonesia
[*]E-mail: liamuliani@gmail.com

Received: 25 November 2020 / *Accepted:* 14 January 2021 / *Published:* 31 January 2021

Dye-sensitized solar cells (DSCs) rely on a photoelectrochemical mechanism. Currently, one of the most significant developments of DSCs is intended toward developing a module for building-integrated photovoltaics (BIPVs). The DSC module could be achieved in a variety of colors and shapes and can perform under relatively low light intensity, making it suitable for solar windows as BIPVs. DSC modules for solar windows must have high transparency in addition to high electrical performance. The transparency of the module can be determined by the materials used and the fabrication process. In this work, we demonstrate the fabrication of a DSC module on transparent conductive glass substrates using a screen-printing method. The module consists of 16 sub-modules that were externally integrated. Each sub-module contained seven grid-type cells that were internally integrated via Z-type series connections. The total active area of the DSC module was 1,120 cm^2. The current–voltage (*I*–*V*) performance of the module was measured using a Keithley 2400 under direct sunlight. The measurement conducted under low light with an irradiation intensity of 80 W/m^2 produced an open-circuit voltage of 75 V, a short-circuit current of 7.2 mA, a maximum power output of 0.301 W, and a power conversion efficiency of 3.37%. These results indicate that the DSC module can be applied as a solar window because it performed well both under direct light and low light intensities. The stability of the module was monitored for 279 days, and the results indicated that the short-circuit current significantly decreased, whereas for the open-circuit voltage, the decrease was less dramatic.

Keywords: dye-sensitized solar module; solar windows; sub-module; current–voltage; power conversion efficiency

1. INTRODUCTION

Solar windows are glass windows that can transmit natural light, provide artistic decoration and also convert solar energy into electricity. Because of the high transparency required, conventional photovoltaic technologies such as silicon-based solar cells cannot be used in solar windows. Dye-sensitized solar cells (DSCs) attract interest because of their reliability and low cost, facilitating their fabrication with no toxic materials, and they can perform well for applications under low illumination [1, 2, 3]. Additionally, DSCs can be fabricated in various colors or shapes [4] and in a transparent form [5], thereby allowing good workability for solar windows as building-integrated photovoltaics (BIPVs). The transparency of a DSC is determined by materials used, for instance, particle size and material thickness [5].

Generally, a DSC is prepared using two transparent conductive oxide (TCO) substrates that are assembled and sealed together in a sandwich configuration. The DSC structure consists of a photoelectrode (PE) side containing a semiconductor oxide and a dye sensitizer and a counter electrode (CE) side containing a metal catalyst. An electrolyte is then added between the two electrodes, which serves as a redox mediator to regenerate electrons. The semiconductor layer in PE is preferably porous and has a large surface area so that many dye molecules can be absorbed, thereby increasing light absorption. Titanium dioxide (TiO_2) is one of the most suitable semiconductor oxide materials for photovoltaics and photocatalysis because it has a wide bandgap (3.2 eV), strong oxidizing ability, and stability against photocorrosion; besides, its preparation is easy and inexpensive [6, 7]. A dye sensitizer serves as a photon absorber that excites electrons. Several types of dye-sensitized materials have been reported [2, 6]. Among them, ruthenium-based dyes are known to be the most efficient photosensitizers, mostly because of their stability [6]. Meanwhile, the CE serves as a catalyst in the reduction-oxidation reaction and transports electrons from the external circuit to the redox electrolyte reaction. The materials that are often used in a CE are platinum (Pt) and carbon (C). Pt is typically preferred as a catalyst material because of its good catalytic activity, high electrical conductivity, high exchange current density, and transparency [6]. However, Pt is a noble metal that has a relatively high cost and limited abundance, making it difficult to use for the commercialization of DSCs. The electrochemical process occurs in the form of a reduction-oxidation reaction using an electrolyte as a mediator. The most common redox mediator used is the iodide/tri-iodide (I^-/I_3^-) couple because it has a low recombination rate [8]. In 2003, Grätzel *et al*. reported a DSC with an efficiency of 10.6%, an open-circuit voltage (V_{OC}) of 0.75 V, and a short-circuit current density (J_{SC}) of 17.77 mA/cm^2 [9]. In 2014, Simon *et al.* produced a DSC with an efficiency of 13%, V_{OC} of 0.91 V, and J_{SC} of 18.1 mA/cm^2 [10].

A single DSC cell typically produces a voltage below 1 V; therefore, to increase the solar cell output for commercial purposes, the DSC cell should be connected in series, parallel, or a combination of the two. The upscaling of solar cells is typically followed by a decrease in efficiency [11]. This is due to the increase in series resistance and reduction in the ratio of the active area. Nevertheless, increasing the scale of the cell is necessary, particularly for electronic applications with high-power requirements. In a silicon solar cell, a solar module is typically produced by connecting single cells using an external connection, whereas in DSCs, the module can be made by integrating individual cells using an internal connection. Several types of internal configurations can be used to fabricate a DSC module (i.e., the monolithic type, the W type, and Z type) [11, 12]. Generally, a module with a series connection achieves a high voltage value but a low current output, whereas a module with a parallel connection obtains a relatively low voltage value but a high current output [3]. Several studies were conducted on fabricating DSCs with a large active area. Nursam *et al.* reported an efficiency of 1.99% from a DSC module with an active area of 70 cm^2 [13]; Mourtzikou *et al*. reported efficiency of 1.6% with an active area of 855 cm^2 [14], whereas Wei *et al.* reported efficiency of 5.86% for a DSC with a module size of 68.4 cm^2 [3].

The aim of this research was to fabricate a DSC module that is scalable for the industrial production of solar windows. The transparent DSC module was made in the form of a grid shape and arranged from several sub-modules internally integrated in series connection. To demonstrate the applicability of our module, the electrical performance of the DSC module was characterized under direct sunlight.

2. EXPERIMENTAL

2.1. Materials

Fluorine-doped tin oxide (FTO) glass substrates with sheet resistivities of 15 Ω/sq (TEC-15) and 8 Ω/sq (TEC-8) and a thickness of 3.2 mm, a transparent TiO_2 paste (18NR-T), a transparent platinum paste (PT-1), an electrolyte solution (EL-HSE), a Ru-complex dye (Z907), a blocking layer paste (BL-1), a hermetic sealant, and Surlyn® thermoplastic were purchased from Greatcell, Australia. Titanium tetrachloride ($TiCl_4$), ethanol (C_2H_5OH, ≥99.8% purity), and isopropyl alcohol (C_3H_7OH, 99.8%) were all synthesis grade and obtained from Merck. The low-temperature silver paste was purchased from Hunan LEED Electronics, Ink Co., Ltd. A transparent acrylic sheet with a thickness of 2 mm and a silicon rubber sealant (Dexton) were purchased for module assembly. All materials were used as received.

2.2. Design and Fabrication of the DSC Sub-Module

Figure 1 presents the DSC sub-module design produced in this work. This DSC module consisted of 16 sub-modules, each with a size of 100 × 100 mm^2, connected in series. Each sub-module contained seven individual grid-type cells that were internally integrated in Z-type series. A sealant with a width of 1 mm and a silver contact with a width of 0.5 mm were placed between cells. The silver paste was used to connect the cells and form a line pattern that was printed between sealant lines. This design used herein was optimized in our previous work [15].

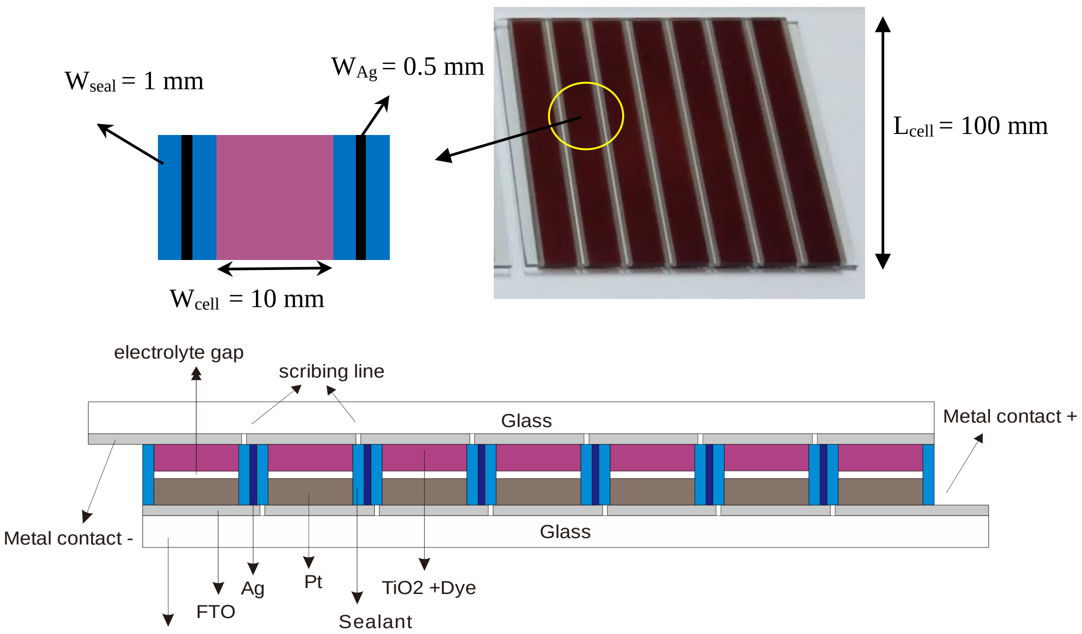

Figure 1. Design of the DSC sub-module showing the top view (top) and cross section of the sub-module (bottom).

The deposition of layers within the DSC sub-modules was conducted using a screen-printing technique. The masking screen was prepared using a screen maker according to the specified designs. Four screen patterns were used for the TiO_2 PE, blocking layer, Ag metal, and Pt CE. First, TEC-15 FTO glass substrates with a size of 100 mm^2 were scribed to remove fluorine-doped tin oxide film to separate individual cells in the DSC sub-module. Then, the scribed substrates were cleaned by soap water, followed by isopropyl alcohol for 10 min in an ultrasonic cleaner, and rinsed by ethanol. The photoelectrode was prepared by depositing a blocking layer paste (BL-1) on the cleaned substrate (pre-treatment). The samples were dried in an oven at 120 °C for 10 min and then annealed in a muffle furnace at 500 °C for 30 min. The process was continued by printing the transparent TiO_2 paste (18NR-T) on top of the BL. The printing was performed twice to get a TiO_2 film with a thickness of ~8–10 µm. The samples were dried in an oven at 120 °C for 10 min after each printing step and then co-fired in a muffle furnace at 500 °C for 30 min. The process was continued by heating the TiO_2 film in 40 mM $TiCl_4$ solution at 70 °C for 30 min, followed by annealing at 500 °C for 15 min (post-treatment). After that, the TiO_2 film was immersed in a solution of Ru-complex dye Z907 in ethanol (20 mg/100 mL) for 24 h at room temperature. The samples were rinsed afterward in ethanol and dried naturally. The CE was prepared by printing a transparent Pt paste (PT-1) on another piece of scribed FTO glass. Similar to the deposition of the TiO_2 paste, the printing of Pt paste was done twice and then dried at 120 °C for 10 min after each printing, followed by co-firing at 450 °C for 30 min. The silver paste was subsequently coated on the CE as a contact grid through a stainless-steel screen. Meanwhile, a sealant with a thickness of 50 µm (Surlyn® thermoplastic) was attached to one of the electrodes (CE). Then, PE and CE were sandwiched and then placed in a hydraulic hot-press at 120°C for several minutes. The completion of the lamination process was confirmed by the disappearance of the melt film boundaries. The liquid electrolyte EL-HSE was injected through a gap between the two electrodes under a vacuum. The electrolyte filled each cell in the sub-module. After that, each DSC sub-module was encapsulated with a hermetic sealant, and the I–V characteristics were then measured.

2.3. Assembly of the DSC Module

Each of the DSC sub-modules was labeled as SM-*X*, where *X* represents the serial number of the sub-module from SM-1 to SM-16. All DSC sub-modules were arranged in series with a four-by-four configuration according to the schematic presented in Figure 2. The sub-modules were connected using external interconnection that is, using cables that were connected to the output terminal of each sub-module. After all DSC sub-modules were connected to form a module, the DSC module was then encapsulated using a transparent acrylic sheet with a size of 160 cm^2 and sealed using silicon rubber. Since the size of the active area for each sub-module was 70 cm^2, the total size of the active area for the whole DSC module was 16 × 70 cm^2 (or 1,120 cm^2).

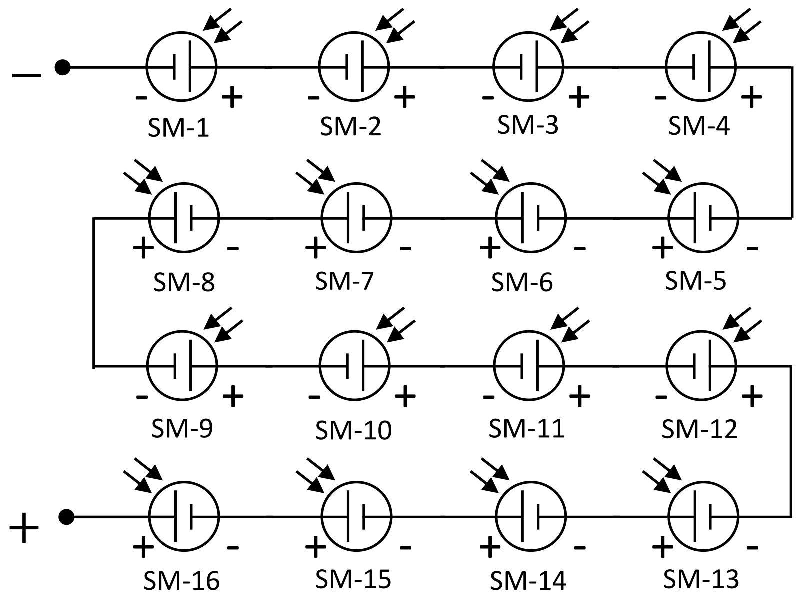

Figure 2. A schematic of the electrical configuration used to connect the DSC sub-modules (SM-1 to SM-16) in series to form the DSC module.

2.4. Characterization

The optical transmittance and absorbance characteristics of materials were measured using Ocean Optics UV-Vis Spectrometer, Maya2000 Pro. The current–voltage (*I*–*V*) characteristics of DSC sub-modules were measured using Keithley 2400. The irradiation was generated by a Xenon light solar simulator (Oriel, Newport USA), which was calibrated using a silicon solar cell as a reference to produce irradiation intensity equal to 1 sun. Meanwhile, the electrical characterization of the DSC module was measured manually using a digital multimeter and a Keithley 2400 source meter under direct sunlight. The irradiation intensity used was varied from 80 to 600 W/m^2. The power conversion efficiency of the sub-modules and the module were calculated using the following equation:

$$\eta = \frac{V_{OC}\, I_{SC}\, FF}{P_{in}} \times 100\%, \qquad (1)$$

where V_{OC} and I_{SC} are the open-circuit voltage (V) and the short-circuit current (A), respectively, *FF* is the fill factor, and P_{in} is the power input (W) received from the irradiation during the measurement.

3. RESULTS AND DISCUSSION

Several aspects should be considered in the fabrication of the DSC module, namely design, material selection, PE and CE preparation, the assembly process, and encapsulation. These aspects significantly affect the electrical performance of the module and the amount of electrical energy produced. Visual appearance is also a factor that is often neglected in solar cells because it is considered trivial. For solar windows, however, visual attractiveness has become a necessity. Herein, the materials used during the fabrication of the DSC module were selected based on the applicability of the module as solar windows. As previously stated, the conductive glass substrate used was FTO with a sheet resistivity of 15 Ω/sq (TEC-15). The consideration of material selection was based on the optical transmittance properties of FTO TEC-15. Two main characteristics of a substrate are essential in a DSC. First, it must be highly transparent (>80%) to allow optimum sunlight through the effective area of the cell. Second, it must have high electrical conductivity to reduce energy loss and allow charge transfer more efficiently. Compared to FTO TEC-8, FTO TEC-15 has a higher sheet resistance than FTO TEC-8, but this drawback is balanced with enhanced optical transmission. Figure 3 illustrates the optical transmittance properties between the two types of FTO glass substrates measured using a UV-Vis spectrophotometer. It can be seen that in the visible region, FTO TEC-15 has a transmittance higher than 80%, whereas FTO TEC-8 has a lower transmittance (below 70%).

PE and CE materials were chosen based on their transparent properties. We used commercial products, namely transparent TiO_2 paste and platinum paste for PE and CE materials, respectively. UV-Vis measurements were conducted to identify the optical transmittance properties of TiO_2 and Pt films. The Pt film has a transmittance higher than 70% in the visible region (i.e., 380–780 nm), whereas for the TiO_2 film, a transmittance of 70% or higher can be obtained at a longer wavelength, i.e., at 470 nm. The optical properties of materials depend on the film thickness: As the film thickness increases, the transmittance value decreases. The thickness of the TiO_2 and Pt films were approximately 8 µm and 3 µm, respectively. Based on the results illustrated in Figure 4, these thicknesses produced sufficient transparency, thereby making the fabricated DSC module suitable for solar window applications.

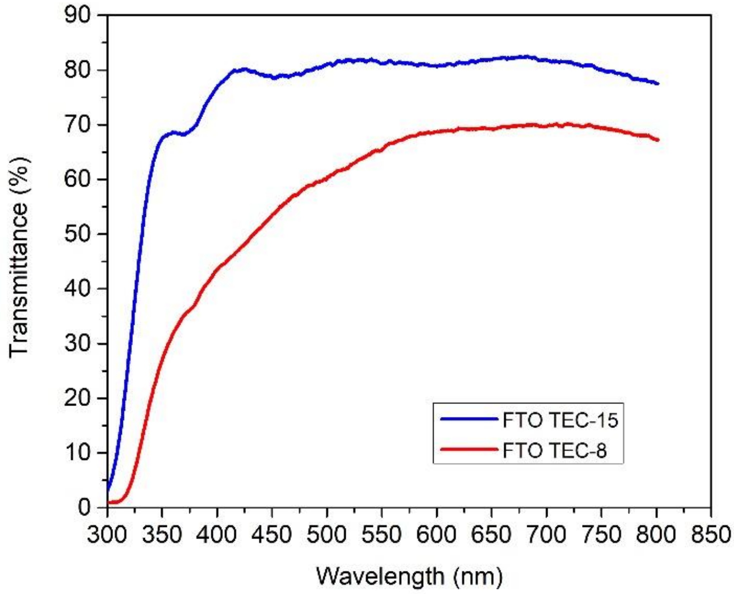

Figure 3. Optical transmittance of FTO TEC-15 with a resistivity of 15 Ω/sq and FTO TEC-8 with a resistivity of 8 Ω/sq.

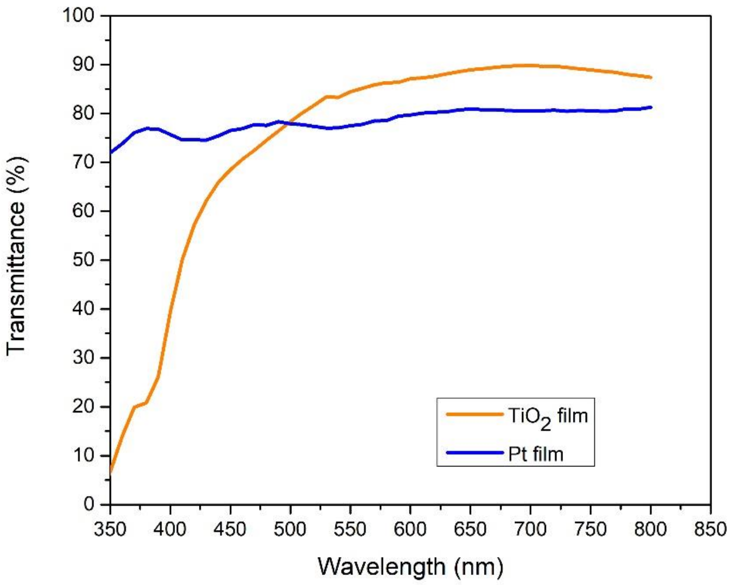

Figure 4. Optical transmittance of the TiO_2 and Pt films on FTO TEC-15.

Ruthenium-based dye Z907 containing 4,4'-dinonyl-2,2'-bypiridine was used as a sensitizer in the fabricated module. Because it is hydrophobic, the dye can sensitize TiO_2 very efficiently and enhance the long-term stability of the module [2]. The dye molecule attached to TiO_2 nanoparticles absorbs incident light. The photons that are absorbed by the dye cause excited electrons and move into the TiO_2 conduction band area.

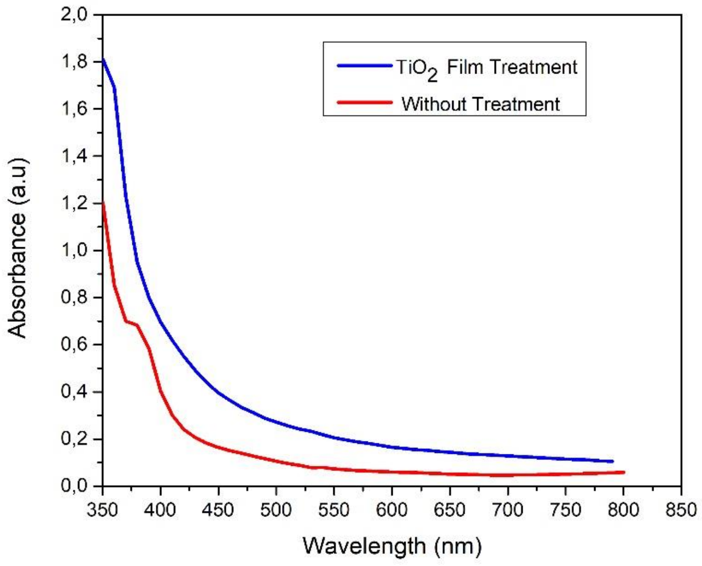

a.

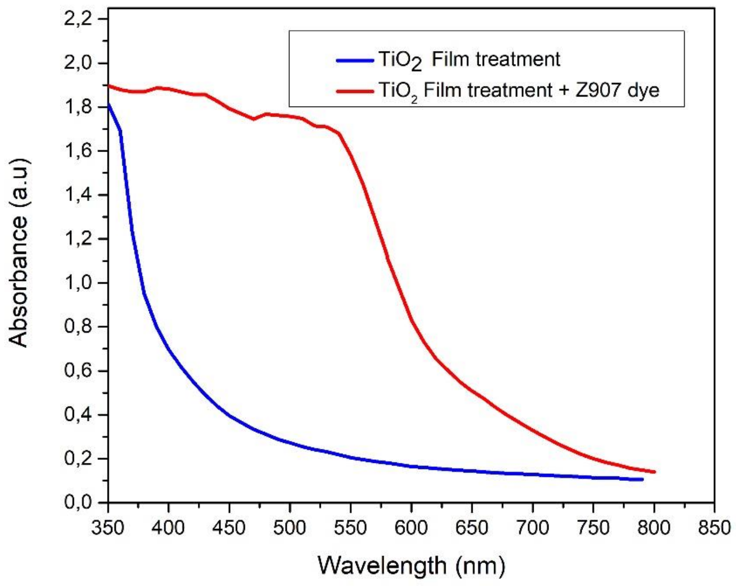

b.

Figure 5. Absorption spectra of the TiO_2 film (a) without and with treatment, (b) without and with sensitization in the Z907 dye.

The preparation of TiO_2 PE was performed in multiple steps. The deposition of the BL on a clean FTO glass surface, or the pre-treatment, was conducted before applying the mesoporous TiO_2 paste. The application of a BL in the DSC has been demonstrated to reduce electron recombination due to electron back transfer from TiO_2 to the electrolyte [17]. Meanwhile, after the deposition of mesoporous TiO_2, a post-treatment step was taken by immersing the TiO_2 film in a $TiCl_4$ solution. This step improves the ability of the TiO_2 photoelectrode to absorb dye molecules so that more photon energy can be captured.

Figure 5(a) presents the light absorption spectra of the TiO_2 film that was without and with treatment (pre- and post-treatment). The light absorption of the TiO_2 film increased after treatment due to the light scattering effect. Figure 5(b) illustrates the influence of dye sensitizer addition to the light absorption of the TiO_2 film with treatment. After treatment, the TiO_2 film became thicker such that the number of dye molecules attached to the TiO_2 film became more abundant; consequently, the number of photons absorbed in the visible light region increased. The positive effect of post-treatment was also confirmed by the I–V characteristics, which were measured on a DSC sub-module (with a total active area of 70 cm^2), as illustrated in Figure 6 and Table 1. These results indicate that the I_{SC} and V_{OC} of the sub-module increased with the amount of post-treatment. The electrical efficiency of sub-module also improved by 20%, wherein the without and the with post-treatment produced an efficiency of 2.86% and 3.47%, respectively.

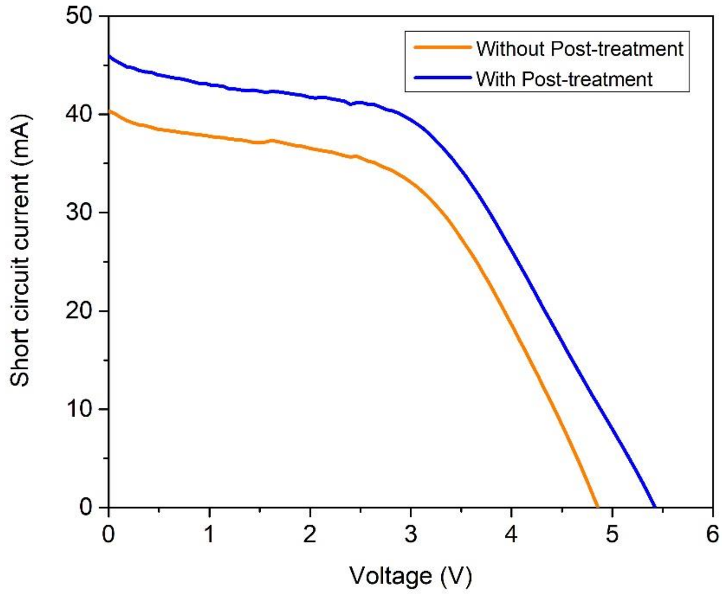

Figure 6. *I–V* curve of the DSC sub-module with the TiO_2 film without and with post-treatment.

Table 1. I–V parameter of the DSC sub-module with the TiO_2 film without and with post treatment.

Type	V_{OC} (V)	I_{SC} (mA)	P_m (W)	*PCE* (%)	*FF*
Without post-treatment	4.86	40.34	0.10	2.86	0.51
With post-treatment	5.46	45.98	0.12	3.47	0.48

Before the sub-modules were integrated into the module, their I–V characteristics were measured under the irradiation of a Xenon light, a solar simulator with a calibrated intensity equal to 1 Sun. The electrical parameters of the sub-modules are summarized in Table 2. It can be seen that the performance of the sub-modules is quite uniform, with an average efficiency higher than 2%, except for SM-13. The highest performance was achieved by the SM-4, which produced an open-circuit voltage (V_{OC}) of 5.46

V, a short-circuit current density (J_{SC}) of 0.66 mA/cm^2, a maximum power output (P_m) of 0.12 W, a fill factor (*FF*) of 0.48, and power conversion efficiency (*PCE*) of 3.47%. The lowest performance was produced by SM-13, with V_{OC} = 5 V, J_{SC} = 0.36 mA/cm^2, P_m = 0.07 W, *FF* = 0.53, and *PCE* = 1.92%. Figure 7 illustrates the I–V curves of the sub-modules with the highest and the lowest performances. According to Carella *et al.*, J_{SC} is related to electron injection yield that depends on the absorption properties of the sensitizer both qualitatively and quantitatively [18]. The low J_{SC} value of this sub-module may be due to the ineffective absorption of light by the dye sensitizer. It was apparent that the TiO_2 film of SM-13 was thinner than the others, so less dye was absorbed; thus, the yield of electron injection and the resulting short-circuit current decreased. Consequently, the sub-module with a low short-circuit current produced a low maximum power output and, in turn, a low *PCE*.

Table 2. Electrical parameters of the DSC sub-module.

Sub-Module	V_{OC} (V)	J_{SC} (A/cm^2)	P_m (W)	*PCE* (%)	*FF*
SM-1	5.10	0.70	0.11	3.06	0.43
SM-2	5.34	0.67	0.11	3.16	0.42
SM-3	5.22	0.69	0.11	3.19	0.44
SM-4	5.46	0.66	0.12	3.47	0.48
SM-5	4.55	0.67	0.10	2.72	0.45
SM-6	4.92	0.62	0.11	3.04	0.50
SM-7	4.86	0.58	0.10	2.86	0.51
SM-8	4.74	0.54	0.10	2.96	0.58
SM-9	5.00	0.47	0.08	2.35	0.50
SM-10	4.80	0.48	0.08	2.21	0.51
SM-11	4.86	0.48	0.08	2.33	0.45
SM-12	4.98	0.56	0.09	2.67	0.40
SM-13	5.00	0.36	0.07	1.92	0.53
SM-14	4.68	0.53	0.07	2.02	0.35
SM-15	4.98	0.60	0.10	2.87	0.40
SM-16	4.62	0.63	0.08	2.40	0.32

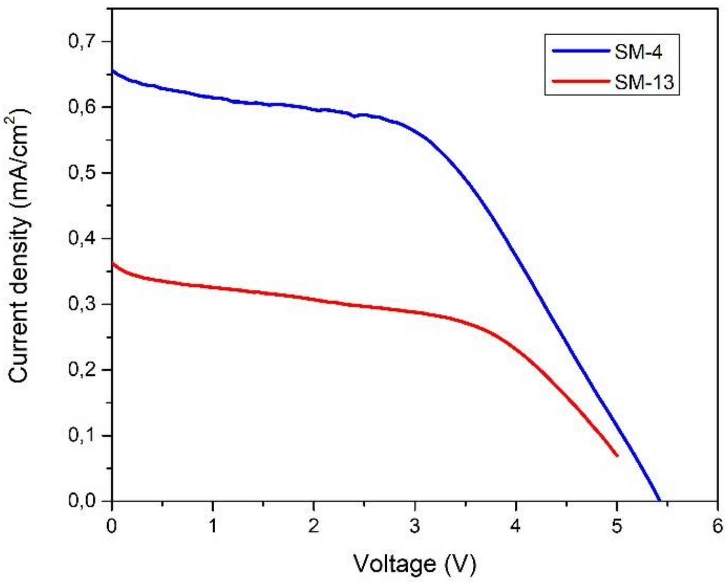

Figure 7. I–V curves of the DSC sub-modules with the highest (SM-4) and lowest (SM-13) performances measured under the solar simulator.

To form a DSC module, the sub-modules were integrated externally in a serial connection and encapsulated using a transparent acrylic sheet with a thickness of 2 mm. Figure 8 presents the prototype of the DSC module resulting in a size of 40 × 40 cm^2 with a total active area of 1,120 cm^2. Unlike the DSC sub-modules, the electrical parameters of the DSC module were measured manually using a digital multimeter and a Keithley 2400 source meter under direct sunlight to ensure sufficient light exposure. The disadvantage of manual I–V measurement is the difficulty in obtaining stable sunlight intensity. Table 3 lists the I–V parameters of the DSC module measured outdoors under various light intensities using a digital multimeter. It can be seen that the open-circuit voltage values were not seriously affected by the light intensity, whereas the short-circuit current and power output were influenced by the light intensity. Generally, the output current increased with the increase in light intensity. When the solar radiation intensity increases, more photons strike the DSC module. With a higher number of photons hitting the surface of the PE, the excited dye molecules and the transfer of electrons into the TiO_2 conductor band increase, resulting in enhanced photocurrent [19]. The power output is equivalent to the light intensity. However, unlike the power output, the power conversion efficiency typically decreases as the light intensity increases as a result of limited electron mass transport [20]. The increasing light intensity can also cause an increase in the temperature, which affects the open-circuit voltage. As the temperature increases, the charge diffusion and, in turn, the charge mobility increase. This consequently leads to an increase in the open-circuit voltage [21].

Figure 8. Photograph of the DSC module prototype for solar windows.

Table 3. I–V parameters of the DSC module measured outdoors under various light intensities.

Parameters	Light Intensity		
	600 W/m^2	200 W/m^2	80 W/m^2
I_{SC} (mA)	59	10	7.2
V_{OC} (V)	83	79	75

Figure 9 displays measurement results of the I–V curve of the DSC module at an intensity of 80 W/m^2. This condition was chosen to demonstrate the ability of the DSC module to operate at low light intensity. The V_{OC}, I_{SC}, and *PCE* of the DSC module (40 × 40 cm^2) under light intensity of 80 W/m^2 were 75 V, 7.2 mA, and 3.37%, respectively. As a comparison, Mourtzikou *et al.* fabricated a similar DSC module with a size of 50 × 50 cm^2, which produced *Isc* = 36 mA, *Voc* = 15.8 V, and *PCE* = 2.1% under light intensity of 210 W/m^2 [14]. Our results have successfully demonstrated the fabrication of a fully transparent DSC module that has excellent electrical performance and the ability to work under both strong and low light conditions. It has been demonstrated that the fabricated DSC module is highly suitable for application as a solar window, which is also visually attractive and has promising electrical properties.

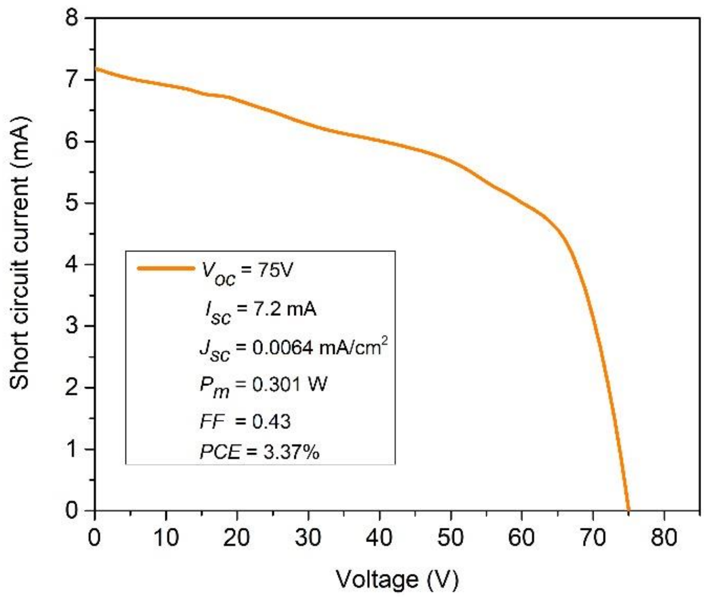

Figure 9. I–V curve of the DSC module measured outdoors under relatively low light intensity (80 W/m^2).

The long-term stability of solar modules is an important factor that needs to be considered, especially for building-integrated applications [11]. The electrical performance stability of the DSC module was monitored for 279 days. To ensure that the DSC module was airtight, all sides of the module were encapsulated using Surlyn® and laminated using a transparent acrylic sheet and silicon rubber. Figure 10 illustrates the short-circuit current and the open-circuit voltage of the DSC module on the 1st, 85th, and 279th days. The measurements were conducted outdoors when the sunlight intensity was ~600 W/m^2. It can be seen that the electrical parameters of the DSC module decreased over time. The short-circuit current decreased significantly on the 85th day (by 88%), from 59 mA to 6.7 mA, whereas the open-circuit voltage only decreased lightly (by 12%), from 83 V to 73 V. On day 279, the short-circuit current and the open-circuit voltage of the module decreased to 0.01 mA and 48 V, respectively. In Figure 10, the DSC module did not indicate good electrical stability. This could be attributed to imperfections in the encapsulation of the DSC module. Such conditions may cause leakages due to pinholes that existed in the sealant, thereby causing the evaporation of the liquid electrolyte. Thus, the amount or volume of electrolytes in the DSC module decreased over time. This phenomenon also increases series resistance (Rs) which result in a decrease in charge and ion mobility. The reduction in the electrolyte had an impact on the inhibition of dye molecule regeneration and electron excitation, therefore causing the photocurrent to drop rapidly. It has been reported that, if not properly encapsulated, liquid electrolytes themselves could cause leaking since their corrosive nature could destroy the metallic interconnection [22]. For solar window applications in BIPVs, making a good encapsulation and developing fewer volatile electrolytes for the DSC module remain major challenges that should be solved to improve the stability of the module.

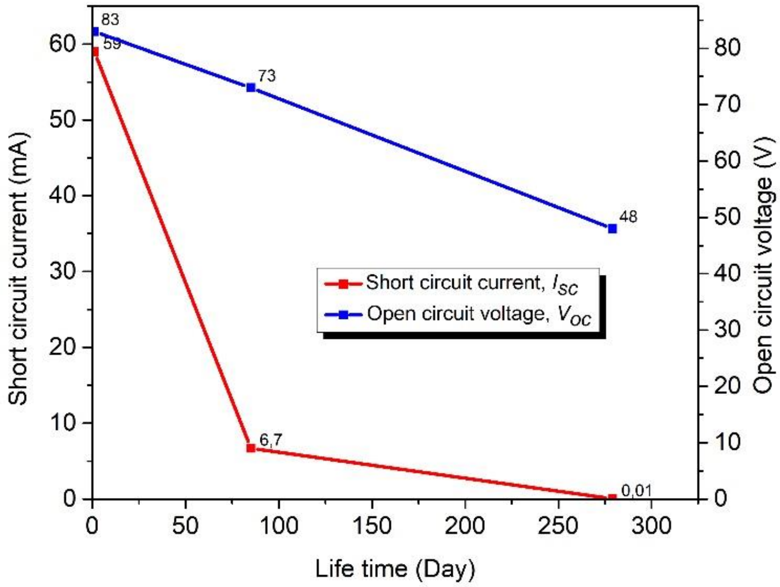

Figure 10. Lifetime characteristics of the DSC module measured under sunlight with intensity of 600 W/m^2.

4. CONCLUSIONS

A transparent dye-sensitized solar module with an area of 40 × 40 cm^2 has been fabricated and characterized. The DSC module was specifically designed for solar window applications. The transparency of the module was achieved by using materials with certain specifications (i.e., FTO with high resistance, transparent Pt, and TiO_2) and tuning the thickness of the films in PE and CE. Our DSC design integrated a grid-type DSC sub-module using Z-type series. This design was simpler and more effective in the printing process of each electrode so that the DSC module can be scaled for industrial production. The I–V characteristics of the DSC module were measured under direct sunlight, and the results indicated that the DSC module could perform both under high and low light intensities (i.e., cloudy days). The stability of the module, however, remains a problem for mass production in the future. This issue could be solved by improving the encapsulation and reducing the volatility of the electrolyte.

ACKNOWLEDGMENTS
This work was supported by the Indonesian Institute of Sciences (LIPI) under DIPA 2019 of the Research Center for Electronics and Telecommunication (P2ET) as part research project entitled *Development of Solar Modules based on Dye-sensitized Solar Cells for Solar Windows Application*.

References

1. B. O'Regan and M. Gratzel, *Nature*, 353 (1991) 737.

2. K. Sharma, V. Sharma and S. S. Sharma, *Nanoscale Res Lett*, 3, 381 (2018) 1.
3. T. C. Wei, S. P. Feng, Y-Huei Chang, S. J. Cherng, Y. J. Lin, C.M. Chen, and H. H. Chen, *Int. J. Electrochem. Sci*, 7 (2012) 11904.
4. J. G. Kang, J. H. Kim, H. B. Jang, and J. T. Kim, *Int J Photoenergy, Research, Article* ID 715427 (2015) 1.
5. A. Roy, A. Ghosh, S. Bhandari, P. Selvaraj, S. Sundaram, and T. K. Mallick, *J Phys Chem*, 123 (2019) 23834.
6. S. Suhaimi, M. M. Shahimin, Z. A. Alahmed, J. Chyský, and A. H. Reshak, *Int J Electrochem Sci*, 10 (2015) 2859.
7. L. Muliani and B. Sunendar, *Adv Mater Res*, 789 (2013) 171.
8. P. Gu, D. Yang, X. Zhu, H. Sun, P. Wangyang, J. Li, and H. Tian, *AIP Advances*, 7-105219 (2017) 1.
9. M. Grätzel, *J Photochem Photobiol C* 4 (2003) 145.
10. S. Mathew, A. Yella, P. Gao, R. H. Baker, B. F. E. Curchod, N. A. Astani, I. Tavernelli, U. Rothlisberger, Md. K. Nazeeruddin and M. Gra¨tzel, *Nat Chem*, 6 (2014) 242.
11. R. Sastrawan., Photovoltaic Modules of Dye Solar Cells, PhD Dissertation, (2006) University of Freiburg, German.
12. G. E. Tulloch, *J Photochem Photobiol A* 164 (2004) 209.
13. N. M. Nursam, J. Hidayat, and L. Muliani, *2017 15th Intl. Conf. QiR: Intl. Symp. Elec. and Com. Eng*, Bali, Indonesia, (2017), 132.
14. A. Mourtzikou, D. Sygkridou, T. Georgakopoulos, G. Katsagounos, and E. Stathatos, *Int J Struct Constr Eng*, 14 (2020) 90.
15. Lia Muliani, Jojo Hidayat, and Lilis Retnaningsih, Dye Sensitized Solar Sub-module, *The 2nd International Conference on Radar, Antenna, Microwave, Electronics and Telecommunications (ICRAMET)*, Batam, Indonesia, (2014) 42.
16. Natalita M. Nursam and L. Muliani, *Int J Technol*, 2 (2012) 129.
17. A. Sedghi and H. N. Miankushki, *Jpn J Appl Phys*, 52-075002 (2013) 1.
18. A. Carella, F. Borbone, and R. Centore, *Front Chem*, 6-481(2018) 1.
19. B. Tripathi, P. Yadav, and M. Kumar, *Int J Photoenergy*, Article ID 646407, (2013) 1.
20. J. H. Kim, K. J. Moon, J. M. Kim, D. Lee, and S. H. Kim, *Sol Energy*, 113, (2015) 251.
21. R. Guliani, A. Jainb and A. Kapoora, *The Open Renew Energy J*, 5 (2012) 49.
22. A. Fakharuddin, R. Jose, T. M. Brown, F. F. Santiagoc, and J. Bisquert, *Energy Environ Sci*, 7 (2014) 3952.

© 2021 The Authors. Published by ESG (www.electrochemsci.org). This article is an open access article distributed under the terms and conditions of the Creative Commons Attribution license (http://creativecommons.org/licenses/by/4.0/).